Low Speed Sensorless Control of an Induction Motor Fed by Multilevel Converter to Reduce Current Distortion

K. Saleh, G.M. Asher, M. Sumner, M. Tomasini, Q. Gao
Department of Electrical and Electronic Engineering,University of Nottingham,Nottingham,NG72RD

Keywords

<<Induction motor, Multilevel converters, Sensorless control>>

Abstract

The paper introduces a new scheme to track the rotor position of an induction motor. The scheme uses the measurement of current derivatives during null switching vectors of a standard PWM scheme and reduces the minimum pulse widths required to allow high frequency switching oscillations to die down. The motor current distortion is therefore also reduced. The method uses H-Bridges connected in series with the main converter. This configuration has the same characteristics as the multilevel converters proposed for high power induction motor drives. The H-Bridges can be used to produce low voltage test vectors during the null vector which can provide a good rotor position estimation with very low additional current distortion. The paper will present experimental results which show the potential capability for sensorless speed control.

Introduction

The estimation of the rotor position through tracking the variation of the motor leakage inductances has been reported in [1,2,3,4,5]. The motor leakage inductance varies due to geometric or saturation saliency, and is used as an indication of rotor or flux position. Techniques such as the INFORM method [1] measure the stator current transient response to specific voltage vectors or "test-pulses". The di/dt measurement can then be used to reconstruct a resolver like signal to track flux or rotor position.

When a new switching vector is imposed onto a motor by switching an IGBT, the switching action excites the parasitic capacitances within the inverter and motor and causes high frequency oscillations in the motor current. Parasitic capacitances to ground (e.g motor winding to case, IGBT to heatsink) cause common mode oscillations and inter phase capacitances (inter-turn in motor) cause differential mode oscillation. The amplitude of the oscillation is related to the size of the voltage switched, and the oscillations may take many microseconds to decay. The oscillation must be completely decayed before the di/dt can be sampled, and therefore these position estimation techniques impose a minimum voltage pulse width t_{min} on the operation of the drive. At low speeds the small active voltages in [3] or test vectors in [1,2] need to be extended to t_{min} for a correct di/dt measurement. This extension for the small active voltage vectors will introduce a large spike into the motor current as described in [3].

A new method for sensorless control is introduced in this paper. In the proposed method, small voltage pulses are applied in the null vector using a separate H-bridge converter and the corresponding di/dt measurements are taken. The method is similar to the INFORM method but introduces additional power circuitry. The H bridge voltages are smaller than the main two level inverter voltage and these small voltage pulses reduce the high frequency differential mode current oscillation. Therefore t_{min} can be shortened. As a result, the motor current distortion can be significantly reduced. The new approach is intended for high power induction motor drives, where multi-level inverter topologies may be used as the main power converter and no additional power circuitry is required as shown in Fig.1.

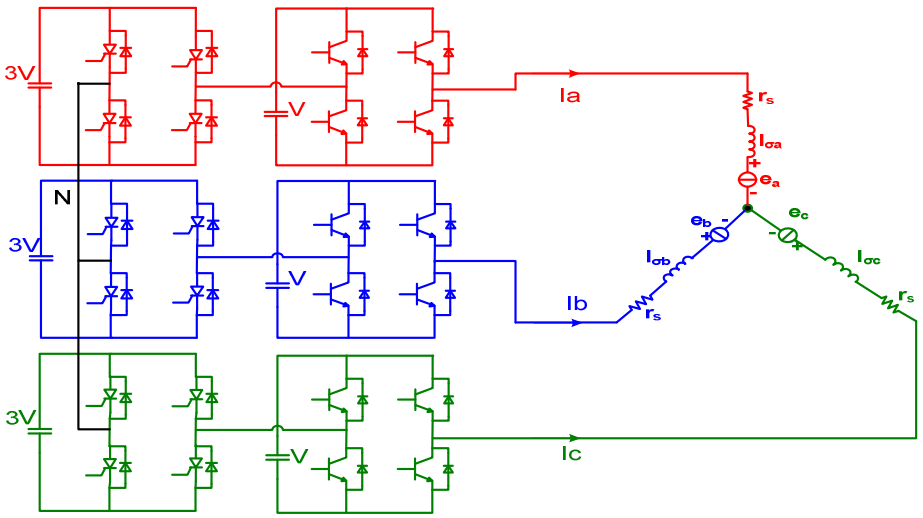

Fig 1: schematic for a true 9 level multi-level H-Bridge converter.

The method has been verified on a low power experimental prototype which can represent the switching pattern of a H bridge type multi-level drive, even if its topology is different to the high power drives proposed in [6,7].

Implementation of a Small Voltage Pulse Using the H-Bridges

Fig 2 shows the schematic for the prototype converter developed for this project [8,9]. To ease development three H Bridges have been connected to a standard inverter. This configuration is designed to evaluate the principle of the method even if it does not use the envisage target topology. It is however anticipated that the method developed here will be applicable to very high power induction motor drives fed from "isolated cell " multi-level converters of Fig. 1. which employ different switching devices and cell voltages as proposed in[6,7] .

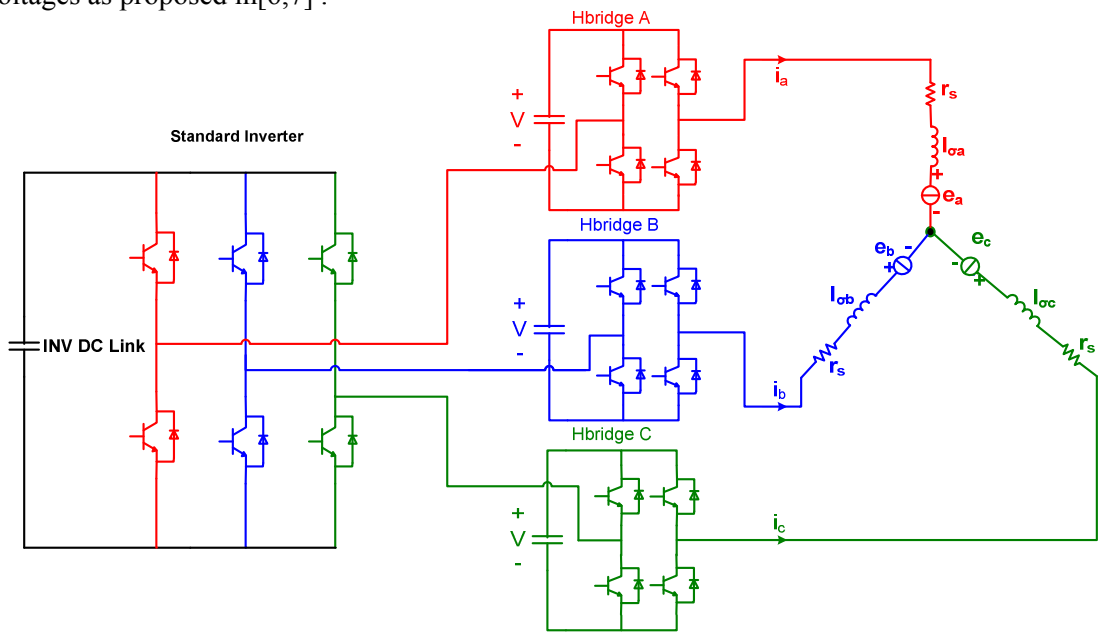

Fig 2: Topology of the prototype multilevel converter topology.

During normal operation, no additional test-pulses are imposed on the machine, and the H-Bridges will have a switching pattern that produces zero volts at their outputs as shown in Fig 3.a i.e. the upper two

IGBTs will be ON. When a positive pulse (+V) is required from a particular H Bridge, to impose a positive "test pulse" on that machine phase winding, the switching pattern of the H-Bridge will be as shown in Fig 3.b. Finally when a negative test-pulse (-V) is required, the H-Bridge will have a switching pattern as seen in Fig 3.c.

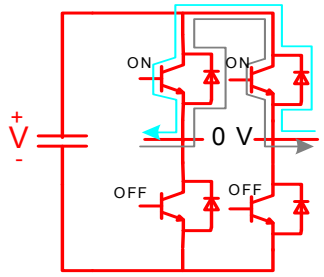

Fig 3.a: H-Bridge switching and current directions to produce 0V output voltage

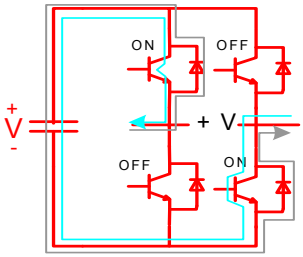

Fig 3.b :H-Bridge switching and current directions to produce +V output voltage

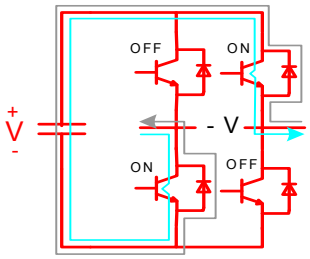

Fig 3.c :H-Bridge switching and current directions to produce –V output voltage

Tracking the Rotor Slotting Saliency Using the H-Bridge Pulses

The stator leakage inductances of the induction motor are modulated by anisotropy either from the rotor slotting or from the saturation of the main flux. The modulation can be expressed by the following equations :-

$$l\sigma a = L_0 + \Delta L cos(n_{an}\theta_{an}) \quad (1)$$

$$l\sigma b = L_0 + \Delta L cos\left(n_{an}(\theta_{an} - \frac{2\pi}{3}\right) \quad (2)$$

$$l\sigma c = L_0 + \Delta L cos\left(n_{an}(\theta_{an} - \frac{4\pi}{3}\right) \quad (3)$$

Where L_0 is the average inductance and ΔL is the variation of leakage inductance due to the rotor anisotropy (n_{an}=2 for saturation anisotropy , and $n_{an} = \frac{N_r}{p}$ for rotor slotting , where N_r is the rotor slot number and p the number of pole pairs).

This modulation of the stator leakage inductances will be reflected in the transient response of the motor line current to the test vector imposed by the H-Bridges as shown in Fig 4. So by measuring the transient current response to the test vector it is possible to detect the inductance variation and track the rotor position or flux angle as shown in the equations below.

When H-Bridge A creates $+V$ test pulse the following equations can be derived using the machine equivalent circuit shown in Fig 1 :-

$$+V = r_s * {i_a}^{(+V)} + l_{\sigma a} * \frac{di_a^{(+V)}}{dt} + e_a^{(+V)} - r_s * {i_b}^{(+V)} - l_{\sigma b} * \frac{di_b^{(+V)}}{dt} - e_b^{(+V)} \quad (4)$$

$$0 = r_s * {i_b}^{(+V)} + l_{\sigma b} * \frac{di_b^{(+V)}}{dt} + e_b^{(+V)} - r_s * {i_c}^{(+V)} - l_{\sigma c} * \frac{di_c^{(+V)}}{dt} - e_b^{(+V))} \quad (5)$$

$$-V = r_s * {i_c}^{(+V)} + l_{\sigma c} * \frac{di_c^{(+V)}}{dt} + e_c^{(+V)} - r_s * {i_a}^{(+V)} - l_{\sigma a} * \frac{di_a^{(+V)}}{dt} - e_a^{(+V)} \quad (6)$$

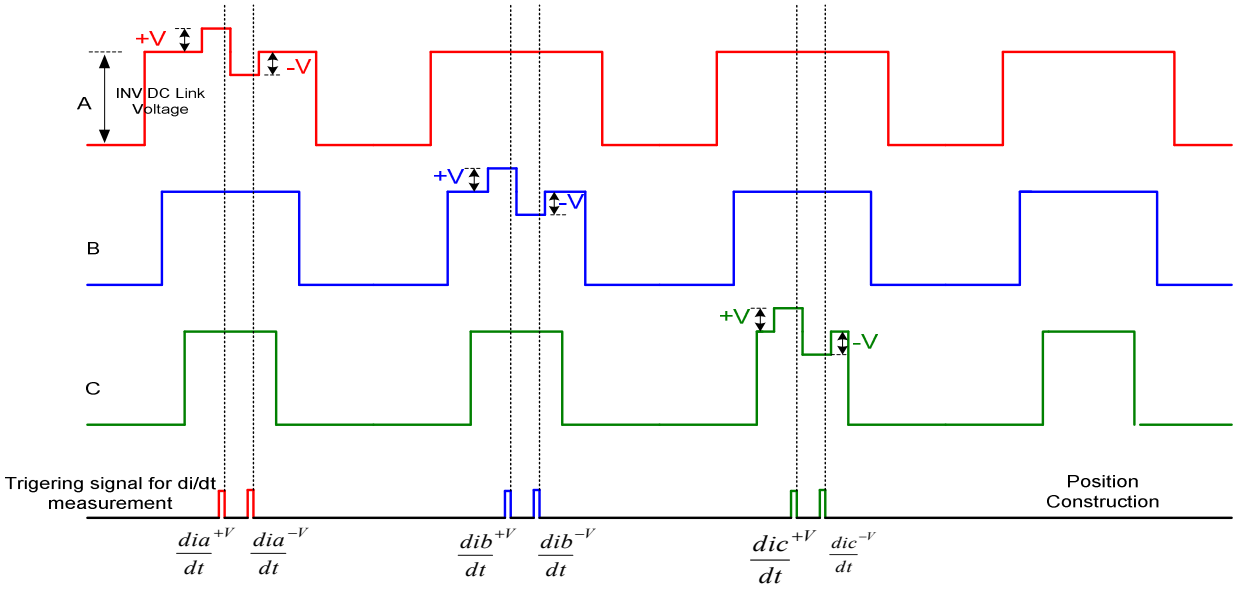

Fig 4: Switching pattern of the multilevel converter drive and the sequence for di/dt measurement and position construction

Where $+V$ is the H-Bridge DC Link voltage, r_s is the stator resistance per phase, and e_a is the back emf in phase a. The superscripts +V etc denote that the measurement is made during the +V test pulse.

In a similar way, when H-Bridge A generates the $-V$ test pulse the following equations can be derived:-

$$-V = r_s * i_a{}^{(-V)} + l_{\sigma a} * \frac{di_a^{(-V)}}{dt} + e_a^{(-V)} - r_s * i_b{}^{(-V)} - l_{\sigma b} * \frac{di_b^{(-V)}}{dt} - e_b^{(-V)} \quad (7)$$

$$0 = r_s * i_b{}^{(-V)} + l_{\sigma b} * \frac{di_b^{(-V)}}{dt} + e_b^{(-V)} - r_s * i_c{}^{(-V)} - l_{\sigma c} * \frac{di_c^{(-V)}}{dt} - e_b^{(-V))} \quad (8)$$

$$+V = r_s * i_c{}^{(-V)} + l_{\sigma c} * \frac{di_c^{(-V)}}{dt} + e_c^{(-V)} - r_s * i_a{}^{(-V)} - l_{\sigma a} * \frac{di_a^{(-V)}}{dt} - e_a^{(-V)} \quad (9)$$

Since the time between applying the $+V$ and $-V$ test vectors is very short, it can be assumed that :-

$$e_a^{(+V)} = e_a^{(-V)}, e_b^{(+V)} = e_b^{(-V)}, e_c^{(+V)} = e_c^{(-V)}$$

Also as the voltage across the stator resistance is small compared to the H-Bridge voltages

$+V$ and $-V$ can also be neglected.

Subtracting equations (7),(8),(9) from equation (5),(6),(7) respectively we obtain the following equations:-

$$+2V = l_{\sigma a} * (\frac{di_a^{(+V)}}{dt} - \frac{di_a^{(-V)}}{dt}) - l_{\sigma b} * (\frac{di_b^{(+V)}}{dt} - \frac{di_b^{(-V)}}{dt}) \quad (10)$$

$$0 = l_{\sigma b} * \left(\frac{di_b^{(+V)}}{dt} - \frac{di_b^{(-V)}}{dt}\right) - l_{\sigma c} * (\frac{di_c^{(+V)}}{dt} - \frac{di_c^{(-V)}}{dt}) \quad (11)$$

$$-2V = l_{\sigma c} * \left(\frac{di_c^{(+V)}}{dt} - \frac{di_c^{(-V)}}{dt}\right) - l_{\sigma a} * (\frac{di_a^{(+V)}}{dt} - \frac{di_a^{(-V)}}{dt}) \quad (12)$$

From equations (10),(12) we derive:-

$$\left(\frac{di_a^{(+V)}}{dt} - \frac{di_a^{(-V)}}{dt}\right) = \frac{+2V(l_{\sigma b}+l_{\sigma c})}{(l_{\sigma a}\, l_{\sigma b}+ l_{\sigma b}l_{\sigma c}+l_{\sigma c}l_{\sigma a})} \tag{13}$$

Substituting $l_{\sigma a}\, l_{\sigma b} + l_{\sigma b}l_{\sigma c} + l_{\sigma c}l_{\sigma a}$ by $3L_0\left(1 - \left(\frac{\Delta L}{2L_0}\right)^2\right)$ we obtain:-

$$\left(\frac{di_a^{(+V)}}{dt} - \frac{di_a^{(-V)}}{dt}\right) = \frac{-2V(2L_0-\Delta L cos(n_{an}\theta_{an}))}{3L_0\left(1-\left(\frac{\Delta L}{2L_0}\right)^2\right)} \tag{14}$$

By defining the constant $g = \frac{3\left(1-\left(\frac{\Delta L}{2L_0}\right)^2\right)}{2V}$

the rotor position scalar for the a phase can then be defined as :-

$$P_a = -2 - g\left(\frac{di_a^{(+V)}}{dt} - \frac{di_a^{(-V)}}{dt}\right) \tag{15}$$

Repeating for phases b and c yields the following equations for position scalars P_b, P_c :-

$$P_b = -2 - g\left(\frac{di_b^{(+V_b)}}{dt} - \frac{di_b^{(-V_b)}}{dt}\right) \tag{16}$$

$$P_c = -2 - g\left(\frac{di_c^{(+V_c)}}{dt} - \frac{di_a^{(-V_c)}}{dt}\right) \tag{17}$$

The final form for the alpha and beta components of the rotor slot position scalar will be :-

$$P_\alpha = P_a - \frac{1}{2}(P_b + P_c) \tag{18}$$

$$P_\beta = \frac{\sqrt{3}}{2}(P_b - P_c) \tag{19}$$

The scalar position signals, Pα and Pβ can be considered to be similar to resolver signals, and the rotor position can be extracted from them using suitable signal processing. They therefore require the measurement of the motor line current derivative at specific instants of time, i.e. the current derivative in response to specific test pulses. However, the physical construction of the motor, cables and inverter introduce parasitic elements which can adversely effect these measurements and this will be considered in the next section.

Improvements to Current Distortion by using H-Bridge Converters

When an IGBT is turned on or off, it can create a high frequency ringing in the measured motor current. Frequencies of around 100kHz and 1Mhz exist due to common mode and differential mode parasitic effects within the machine such as interwinding capacitance of the motor, capacitance between the IGBT and the heatsink etc. they are also related to the size of the voltage switched by the IGBT. These oscillations decay within a few microseconds, but the consequence is that accurate di/dt measurements can only be made once these oscillations have died down. If the method described in [3] were to be imposed using just the standard inverter, short active vectors must be extended to 25us. This is the minimum time required for the oscillations to decay and this causes severe motor current distortion. By using the additional low voltage H-Bridges pulse during the periods when the active vectors are short, the dv/dt can be reduced as well as the differential mode current oscillation and the current distortion. This is the key benefit from using the additional H Bridges.

Fig 5 and Fig 6 show the current distortion using the method described in [3] and the current distortion using the proposed method. Fig 4 shows the imposition of a minimum pulse vector time – the extension of the pulse to t_{min} followed by the compensation of the extension in the second half of the PWM cycle.

Fig. 6 shows the proposed method for multi-level systems employing short test vectors during the main inverter null vectors. The current ripple is reduced from 3 A peak value using method in [3] to about 1 A peak using the proposed method.

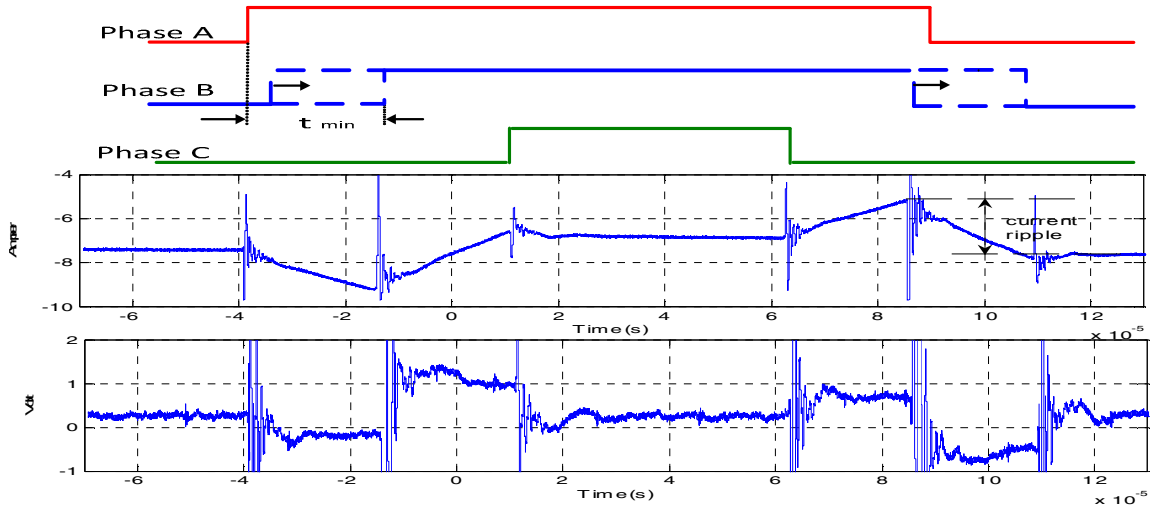

Figure 5 .Top: Normal Two level inverter switching pattern , Middle: motor line current response
Bottom: Measured di/dt over one PWM period using the method described in [3]

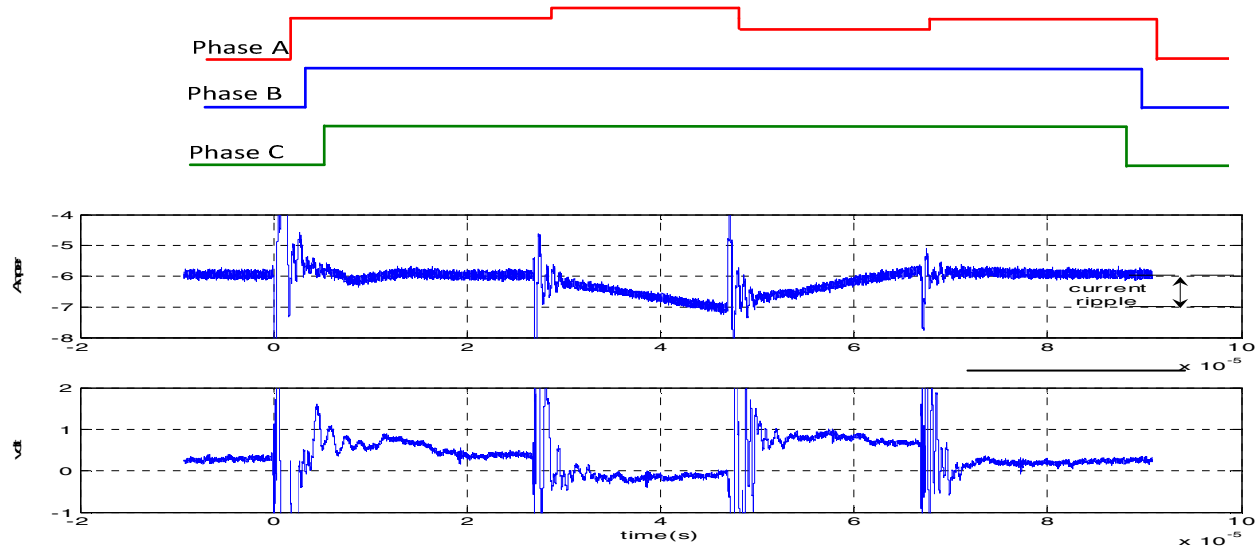

Fig 6 Top: Inverter +H-Bridge switching , Middle : motor line current response
Bottom: Measured di/dt over one PWM period using the proposed method

Reducing the excitation voltages for di/dt measurement from 620 volt in the standard inverter to a lower voltage using H-bridges, the proposed method is able to reduce the current ripple. But at the same time it will reduce the signal to noise ratio (SNR) of the di/dt signal measured and hence affect the quality of the position estimation. To overcome this problem a novel current derivative sensor is used in this work. The new di/dt sensor improves the sensitivity up to 25 times over the old transformer-type di/dt sensor used in [3], and hence increase the SNR. The details about the construction of the new di/dt sensor and it's behaviour compared to other di/dt sensors used before can be found in [10].

From the experiments, it's found that a 150V voltage on the H-Bridge DC link will produce an acceptable di/dt signal that can be used in a full sensorless system in addition to the improvement in the current distortion as will be seen in the next sections.

Estimated Rotor Position and Disturbance Filtering

The anisotropy caused by the rotor slotting using the proposed method is tracked by measuring di/dt in response to test vectors. The position signals $P\alpha$ and $P\beta$ for the experimental system descried in the next section obtained using equations (18) and (19) are show below :-

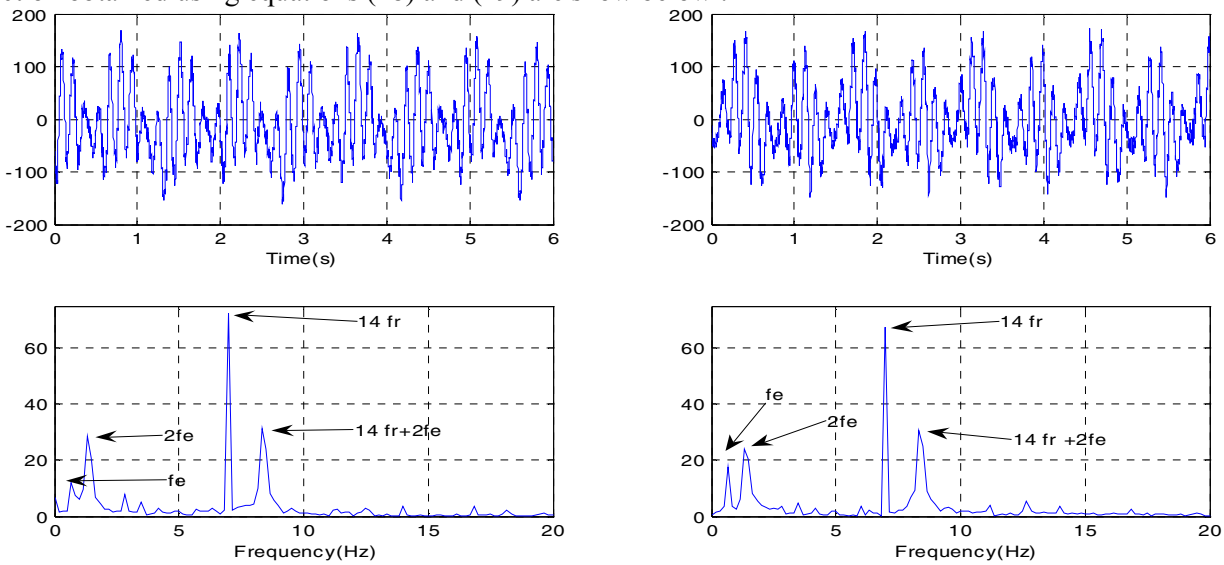

Fig 7 Top: α (left) and β (right) components of the estimated position signal at 15 rpm ,50% load
Bottom: Frequency spectrum of α (left) and β (right) components of the estimated position

Beside tracking the rotor slot salincy ($14\,f_r$) , other disturbance harmonics are observed that make the position signals difficult to use as can be seen from the Fig.7. The ($2f_e$) and (f_e) component are due to the saturation in the machine , and the component ($14f_r + 2f_e$) arises because the position signal ($14f_r$) is modulated by the saturation in the machine ($2f_e$).
To remove the ($2f_e$) and (f_e) components, a low memory disturbance elemination method [11] is used which assumes that these components will vary due to the load conditions only, and is independent of the speed .and so these disturbances can be stored in a memory as a function of Iq only , The filtering of the disturbace ($14f_r + 2f_e$) is achieved by using downstream synchrnous filter in the rotating frame $14\theta_r + 2\theta_e$[12,13] as shown in figure below .

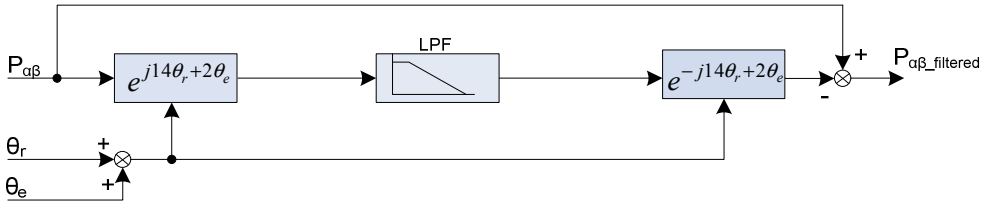

Fig 8 Schematic of the side band filter

Where $P_{\alpha\beta}$ are α and β components of the estimated position signal before filtering ($14f_r + 2f_e$) component ,while $P_{\alpha\beta\text{-filtered}}$ is the filtered signal of the estimated position signals.

The position signals after filtering are shown in Fig. 9. It can be seen that the rotor slotting effect is now much stronger and is now suitable for rotor position tracking.

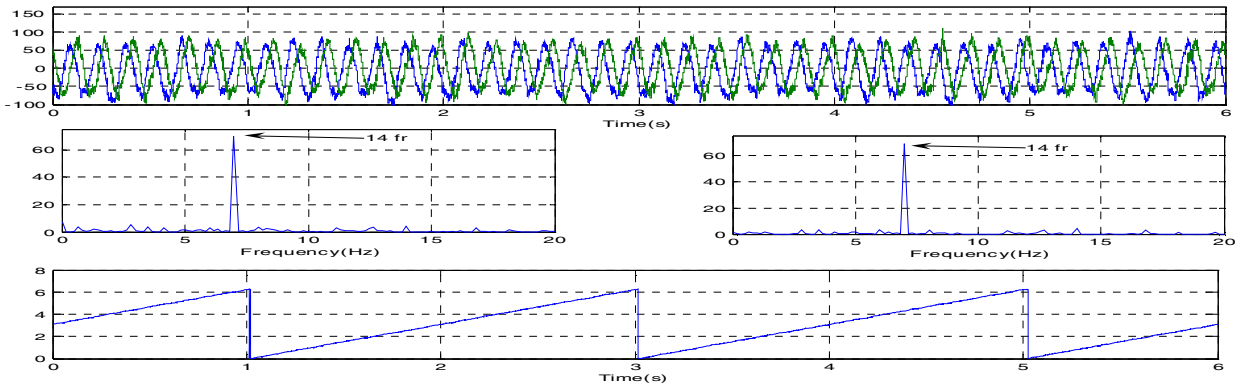

Fig 9 Top: filtered α and β component of the estimated position at 15 rpm ,50% load
Middle: FFT of α (left) and β (right) component of the estimated position
Bottom :-estimated rotor position

The quality of the estimated position signal shown in the figure above is good enough to be used in a complete sensorless system as will be described in the next section.

Experimental Results

The proposed method has been implemented on an Indirect Rotor Field Orientation (IRFO) controlled squirrel cage , star connected , 4 pole ,16 kW , 28 rotor slots, and 50 Hz induction motor ,the switching frequency of the main Inverter was 5 kHz, and the H-Bridges DC Link voltage used in the experiment was 150 Volt. The width of the H-Bridge test vectors were 20 us. And the rated current for the H-Bridges was 80% of the machine rated current and so the load that can be applied to the machine is 50% of the rated load for the safety of the H-Bridges .

After filtering the raw position signals from the disturbances, the α and β component of this position signal is used with a mechanical observer as described in [14]. The estimated rotor position and speed are then used in the field orientation and speed feedback for a sensorless speed control system as shown in Fig 10 .

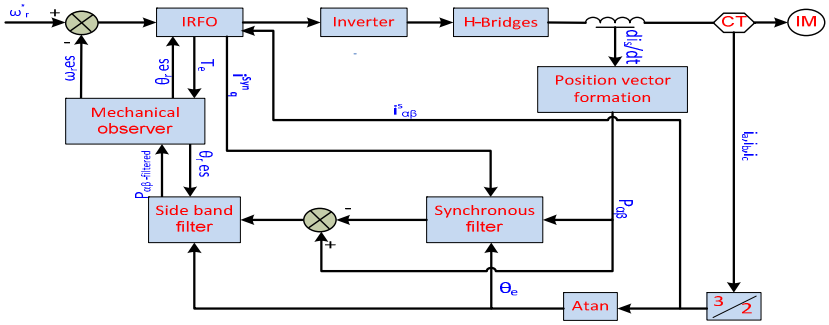

Fig 10 System setup of the sensorless speed control

Figures 11,12,13 show the results of full sensorless speed control under no load and loaded conditions using the proposed method . In Fig 11 a speed step change from 300 to 0 back to 300 rpm at no load was demanded. The estimated speed and position seen in the figure proved that the system responded to the speed steps with good dynamic response and good steady state behaviour. In Fig 12 speed steps between 12 and -12 rpm were applied to the system at no load, and the speed and position response of the system measured through the encoder for evaluation. The results show that the system can work with acceptable performance at low speed as well as at high speed. Finally, in Figure 13, speed step changes between 30 and 0 rpm with 50% load applied to the system are shown. Again the speed measured from the encoder shows a good speed response. The results above show that the system can work in full sensorless speed

control at higher frequencies as well as at low frequencies with and without load using the proposed method.

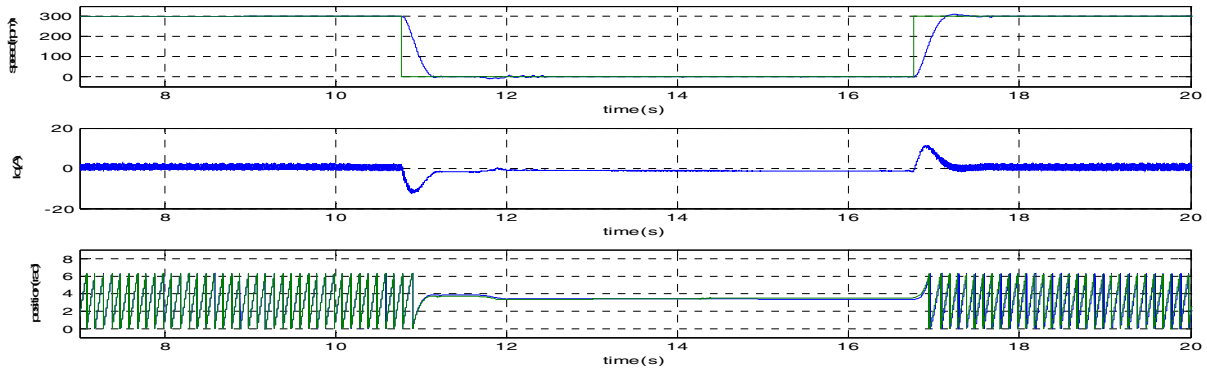

Fig 11 Fully sensorless speed control at no load using the proposed method
Top : reference speed (green) and measured speed (blue) , Middle: Iq
Bottom: measured rotor position (green) and estimated rotor position (blue)

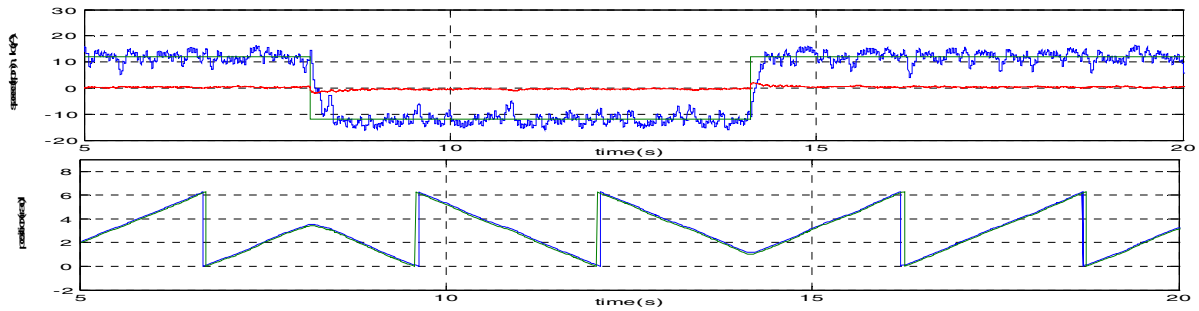

Fig 12 Fully sensorless speed control at no load using the proposed method
Top : reference speed (green) , measured speed (blue), Iq(red)
Bottom: measured rotor position (green) and estimated rotor position (blue)

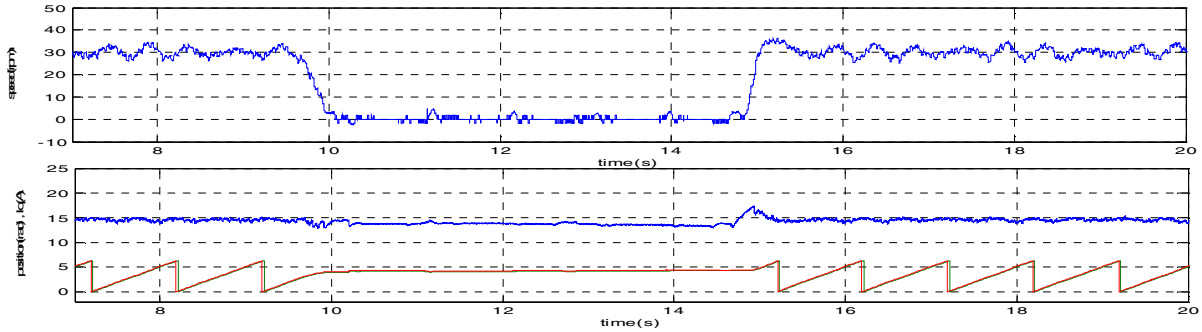

Fig 13 Fully sensorless speed control at 50% Load using the proposed method
Top : measured speed (blue)
Bottom: Iq(blue) , measured rotor position (green) and estimated rotor position (blue)

Conclusion

This paper has outlined a new scheme for rotor position estimation for an induction motor using low voltage H-Bridges connected in series with a standard two level inverter to generate test vectors. The aim here is to reduce the current ripple associated with the minimum active pulse width extension required by INFORM or fundamental PWM based methods used on two level inverter drives, and this is achieved by reducing the excitation voltage from 620V in the standard inverter to 150V using the H-bridges .

Although reducing the excitation voltage improves significantly the current ripple it will also have an effect on the di/dt measurement. i.e decrease the signal to noise ratio (SNR). This challenge is overcome by using the new di/dt sensors introduced in [10].

Experimental results demonstrate the behaviour of the fully speed sensorless control at low speed and higher speed at different load conditions. These results show an acceptable dynamic response and good steady state behaviour.

The paper has demonstrated the viability of using additional H bridges for sensorless induction motor control. The cost of this approach will be prohibitive for low to medium power drives. However, high power induction motors are now being constructed using multi-level inverters, and therefore the techniques described here are very suitable to this class of drives.

References

[1] Manfred Schroedl : Sensorless control of AC machines at low speed and standstill based on the INFORM method , IEEE IAS Annual Meeting, 1996, pp. 270-277

[2] Joachim Holtz and Jorge Juliet : Sensorless Acquisition of the Rotor Position Angle of Induction Motors With Arbitrary Stator Windings , IEEE Transactions on Industry Applications VOL 41 , NO. 6, 2005 , pp 1675-1682

[3] Gao Qiang, Asher.G.M, Sumner.M and Makys.P : Position Estimation of AC Machines at all Frequencies using only Space Vector PWM based Excitation, The 3rd IET International Conference in The Contarf Castle, Dublin, Ireland ,Mar .2006 ,pp . 61-70

[4] E. Robeischl , M. Schroedl :Optimized INFORM Measurement Sequence for Sensorless PM Synchronous Motor Drives With Respect to Minimum Current Distortion. IEEE Transactions on Industrial Applications, no. 2, vol. 40, March/April 2004

[5] C. Spiteri. Staines, G. M. Asher and M. Sumner: Sensorless Control of Induction Machines at Zero and Low Frequency using Zero Sequence Currents , IEEE IAS Annual Meeting, 2004

[6] Manjrekar.M.D , Steimer . P.K , Lipo. T.A: Hybrid multilevel power conversion system: a competitive solution for high-power applications, IEEE Transactions on Industry Applications VOL 36, Issue 3, 2000 pp 834 - 841

[7] Kouro. S , Bernal . R , Miranda . H , Silva . C . A.; Rodriguez, J.: High-Performance Torque and Flux Control for Multilevel Inverter Fed Induction Motors, IEEE Transactions on Power Electronics , VOL 22, Issue 6, 2007, pp 2116 - 2123

[8] Kempski. A , Smolenski . R , Kot . E: Mitigation techniques of conducted EMI in multilevel inverter drives , Compatibility in Power Electronics, IEEE, 2005 , pp 218 - 222

[9] Dae-Wook Kang , Yo-Han Lee , Bum-Seok Suh , Chang-Ho Choi , Dong-Seok Hyun: An Improved Carrier-Based SVPWM Method Using Leg Voltage Redundancies in Generalized Cascaded Multilevel Inverter Topology. IEEE Transactions on Power Electronics ,Volume 18, Issue 1, 2003 Page(s):180 - 187

[10] Matteo Tomasini , Silverio Bolognani : Innovative control algorithms for electric drives – Time optimal current and torque control of IPM SM drives and experimental rig to test a rotor anisotropy-based sensorless vector control of IM drives January 2007, PhD thesis, University of Padua, Italy

[11] Makys, P, Asher G M , Sumner M , Gao Q and Vittek J : A low memory disturbance elimination method for sensorless control of induction motor drive using test vector injection , IECON 2006 ,pp .1071-1076 .

[12] J. Holtz and H. Pan: Elimination of Saturation Effects in Sensorless Position Controlled Induction Motors , IEEE IAS Annual Meeting, Pittsburgh, Oct. 13-18, 2002

[13] Qiang Gao, Greg Asher and Mark Sumner : Sensorless Position and Speed Control of Induction Motors Using High Frequency Injection And Without off-line Pre- Commissioning , the 31st Annual Meeting of IEEE, IES 2005

[14] Robert D. Lorenz , Keith W. Van Patten : High-Resolution Velocity Estimation for All-Digital, ac Servo Drives , IEEE Transactions on Industry Applications VOL 27, Issue 4, 1991 pp 701 - 705